Extraction and characterization of nanocellulose structures from raw cotton linter

João Paulo Saraiva Morais [a,*], Morsyleide de Freitas Rosa [b], Men de sá Moreira de Souza Filho [b], Lidyane Dias Nascimento [a], Diego Magalhães do Nascimento [b], Ana Ribeiro Cassales [b]

[a] Embrapa Algodão, Rua Oswaldo Cruz, 1143, CEP 58428-095 Campina Grande, PB, Brazil
[b] Embrapa Agroindústria Tropical, Rua Dra. Sara Mesquita, 2270, CEP 60511-110 Fortaleza, CE, Brazil

ARTICLE INFO

ABSTRACT

This study aimed to characterize nanocellulose extracted from cotton (*Gossypium hirsutum*) linters. The nanocellulose was subjected to electronic microscopy, thermal analysis, X-ray diffractometry, light scattering, and contact angle. The properties of the nanocellulose are considerably different from the linter. The acidic hydrolyses applied to extract the nanocrystals increased the crystallinity index and the hydrophilicity and decreased the thermal stability. On average, the nanocrystals were 177 nm long and 12 nm wide, with an aspect ratio of 19 when measured by microscopy. The light scattering results were coherent with the crystal dimensions. Cotton linter is a potential source of nanocellulose crystals, particularly to be used in the production of hydrophilic nanocomposites. Extraction of nanocellulose from raw cotton linter does not require pulping.

© 2012 Elsevier Ltd. All rights reserved.

1. Introduction

Linter is an important by product of the textile industry. Cotton linter is the short fiber that cannot be used in the textile process. When the regular cotton fibers are extracted in the ginning process, the linter remains attached to the seed coat. The fuzzy seed needs to be subjected to an additional process that will mechanically remove the linter. The amount of linter produced worldwide is around 2.5 million metric tons, considering the 42 million metric tons of cotton lint produced in 2010 (FAOSTAT, 2012; Sczostak, 2009). Traditional products made from linter are: absorbent cotton, special papers, cellulose nitrate, and acetate (Sczostak, 2009; Vieira, Beltrão, Lima, & Leão, 2008). In some cases, the linter is not extracted, but kept with the seed (when it is used for oil extraction) or chemically dissolved (for planting the seed).

Producing cellulose nanocrystals is an interesting use for linter. Nanocrystals of cellulose, with diameters ranging from 2 nm to 20 nm and length ranging from 100 nm to 2.1 μm are called whiskers, nanowhiskers, or nanofibrils, and they can be obtained from many natural fibers (Capadona et al., 2009; Pandey, Ahn, Lee, Mohanty, & Misra, 2010; Rosa et al., 2010). Natural fibers are used because they are cheap, abundant, renewable, and biodegradable

(Eichhorn et al., 2010; Siqueira, Bras, & Dufresne, 2009; Teixeira et al., 2010). Nanocrystals can be used as fillers in composites (Capadona et al., 2009; Eichhorn et al., 2010; Stelte & Sanadi, 2009; Teixeira et al., 2010) because they have interesting mechanical properties such as low gas permeability (Stelte & Sanadi, 2009) and stiffness enhancing capacity (Pääkkö et al., 2008). They can also be used as reinforcements for adhesives, components of electronic devices, biomaterials, foams, aerogels, and textiles (Eichhorn et al., 2010; Pääkkö et al., 2008; Pandey et al., 2010; Ummartyotin, Juntaro, Sain, & Manuspiya, 2012).

Crystalline and amorphous regions are found in cellulose fibers in proportions that vary among plant species. For that reason, the characteristics (particularly the dimensions) of nanocellulosic materials depend largely on the raw material. Even though all cellulose nanocrystals are made of the same biopolymer, different raw materials can be used to obtain nanowhiskers tailored to specific needs (Beck-Candanedo, Roman, & Gray, 2005; Eichhorn et al., 2010; Pandey et al., 2010; Rosa et al., 2010).

Cotton fiber is a traditional source of cellulose nanostructures (Rånby, 1949), but its chemical composition can be influenced by many factors including the genotype and the environment where it was produced. However, in the literature on cotton nanocrystals there is scarce information on how and where the cotton was produced (Ibrahim, El-Zawawy, & Nassar, 2010; Lin, Chen, Huang, Dufresne, & Chang, 2009). The use of regular cotton fiber can also result in a product different from those made of linter (Ass, Ciacco, &

Frollini, 2006; Teixeira et al., 2010; Yang, Fukuzumi, Saito, Isogai, & Zhang, 2011). The knowledge on basic properties of the raw material is important for the reliable use of these nanostructures. This study aimed to extract and characterize cellulose nanowhiskers obtained from raw cotton linter produced in Brazil.

2. Materials and methods

2.1. Raw material

The sample was obtained from cotton cv. Delta Opal, harvested in 2010 at Luis Eduardo Magalhães, State of Bahia, Brazil, under environmental conditions of Cerrado (Brazilian Savannah) and Köppen climatic classification BSh (Castro et al., 2010). A first-cut linter was used because it is a cleaner material than second-cut or mill-run linters.

2.2. Nanowhiskers preparation

The linter was ground in a Wiley mill and hydrolyzed without any chemical pretreatment. The method of acidic hydrolysis (Cranston & Gray, 2006; Medeiros et al., 2008; Orts et al., 2005) was applied with minor adaptations. The linter was mechanically stirred at a ratio of 1:20 (w/v) of aqueous concentrated sulfuric acid (60%, w/w) with a Teflon© bar dispersing element, at 45 °C, for 60 min. The nanowhiskers suspension was centrifuged for 15 min at 13,000 rpm in a High-speed Refrigerated Centrifuge CR22GIII, and the precipitate was resuspended in distilled water and dialyzed with tap water until a pH (6–7) was reached. The process from centrifugation through dialysis was repeated three times.

2.3. Chemical characterization

The content of moisture, ash, extractives, lignin, hemicellulose, and alpha-cellulose was measured in the raw linter (TAPPI, 1993, 2000, 2002a, 2002b, 2009; Yokoyama, Kadla, & Chang, 2002). The results are presented in wet basis.

2.4. Electronic microscopy

The morphology of cotton linter was analyzed by Scanning Electronic Microscopy. The fibers were ground in a Wiley mill and oven-dried at 40 °C for 24 h. They were gold-coated for 15 min in Emitech K550 metalizer with argon as a carrier gas. The metalized linter was scanned in a Zeiss DSM 940A SEM under accelerated electrons with 15 kV of energy. The width of 31 individual fibers was measured, and the mean, standard deviation, and confidence interval were calculated.

The dimensions of the nanocellulose whiskers were measured by transmission electronic microscopy (TEM). The nanocellulose suspension at 4% (w/v) was mildly ultrasonicated in a water bath sonicator for 30 min, and 1 mL of the solution was dropped on a 300 mesh nickel grid coated with Formvar© polymer. After 2 min, the excessive water was drained with a Wathman paper no. 2, and the grid was inverted and allowed to touch a drop of uranyl acetate 2% (w/v) for 5 min. This process was repeated three times, and the grid was air-dried at room temperature for 24 h.

The grid was analyzed in a Morgani 268D TEM, with 0.2 nm of resolution. The length and width of 100 crystals were measured using the software Gimp 2.6. The mean, standard deviation, and confidence interval were calculated.

2.5. Thermal analyses

The thermal stability of the raw linter and nanowhiskers was analyzed in a Mettler Toledo TGA/SDTA 851. Samples weighing 5 mg were analyzed under a nitrogen atmosphere with 50 mL/min of gas flow rate, heating rate of 10 °C/min, and a temperature range from 25 to 800 °C.

2.6. FTIR analyses

FTIR experiments were conducted using an Agilent Cary 640 FTIR spectrometer. Linter sample was dried, ground and pelletized using KBr (1:100, w/w). Nanocellulose suspension 4% (w/v) was added to KBr. The mixture was oven-dried at 65 °C overnight and pelletized. The spectra were recorded in the range from 4000 to 400 cm^{-1} at 4 cm^{-1} resolution and 100 scans per sample.

2.7. X-ray diffractogram

The X-ray diffraction of the materials was measured in a Xpert MDP diffractometer with Co tube at 40 kV and 30 mA. The crystallinity index (ICr) of the cellulose was calculated using the Eq. (1):

$$\%ICr = \left(1 - \left(\frac{I_{am}}{I_{002}}\right)\right) \times 100 \tag{1}$$

in which, I_{am} is the intensity of diffraction of the amorphous material taken at a 2θ angle between 21° and 22°, when the intensity is minimal, and I_{002} is the maximum intensity of diffraction of the (0 0 2) lattice peak at a 2θ angle between 26° and 27° (Segal, Creely, Martin, & Conrad, 1959).

2.8. Contact angle

A drop of water was placed on the surface of raw linter, glass, and nanocellulose coated glass. For the raw linter, a layer of about 5 cm^2 of surface and 0.5 cm thick was hand-molded, and the water drop was applied. The contact angle was measured on glass applying a water drop on a 26 mm × 76 mm microscopy glass slide. For the nanocellulose, 1 mL of the whisker suspension at 4% (w/v) was dripped upon the glass slide. Another slide was used to spread the suspension evenly over the whole surface, and the glass slide was oven-dried at 60 °C for 5 min. The measurement was made when the slide reached room temperature.

The contact angle was measured with a lab-made software, with seven replications of two preparations of each material. Statistical analysis was performed by the software SisVar© considering a completely randomized design.

2.9. Particle size measurement and zeta potential

The nanocellulose suspension at 4% (w/v) was diluted in water at the ratio of 1:100 (v/v) and ultrasonicated for 30 min in an ultrasonic bath Unique, model USC-1400 (40 kHz of ultrasound frequency, 135 W RMS power). Measurements were made using a Malvern 3000 Zetasizer NanoZS (Malvern Instruments, UK). This equipment uses dynamic light scattering to measure the diffusion of particles moving under Brownian motion, and converts this to size and size distribution. It also uses laser doppler microelectrophoresis to apply and electric field to the dispersion of particles, which then move with a velocity related to their zeta potential. The particle size was measured using the Smoluchowski algorithm.

3. Results and discussion

3.1. Chemical characterization

The cotton linter has an excess of 80% of holocellulose, and more than 3/4 of it is alpha-cellulose (Table 1). This cellulose content is

Table 1
Lignocellulosical composition of cotton linter cv. Delta Opal.

Component	Content (%, w/w)[a]
Moisture	6.33 ± 0.06
Ashes	2.32 ± 0.04
Extractives	5.59 ± 1.91
Insoluble lignin	0.68 ± 0.35
Holocellulose	81.51 ± 4.12
Hemicellulose	4.60 ± 0.60
Alpha-cellulose	76.91 ± 7.19

[a] Mean ± standard error.

within the normal range for cotton linter (Sczostak, 2009), and it is compared to the cellulose content of naturally colored cotton, which ranges from 74.0% to 80.3% (Teixeira et al., 2010). However, it is lower than the 97.7% of cellulose found in hydrophilic (medicinal) cotton.

The linter is an attractive source of nanowhiskers because it has more cellulose than other natural fibers commonly used such as: sisal (*Agave sisalana*) (67–78%) (Oksman, Mathew, Långström, Nyström, & Joseph, 2009), banana (*Musa* spp.) (54–64.4%) (Cherian et al., 2008; Oksman et al., 2009), sugarcane (*Saccharum officinarum*) bagasse (44.9–45%) (Cerqueira, Rodrigues Filho, & Meireles, 2010; Zhao, Wang, & Liu, 2008), bamboo (*Bambusa* spp.) (41.8–54.0%) (Ardanuy, Claramunt, García-Horta, & Barra, 2011; Chen, Yu, Liu, Hai, & Zhang, 2011), and coconut (*Cocos nucifera*) husk (32.5–45.9%) (Brígida, Calado, Gonçalves, & Coelho, 2010; Rosa et al., 2010). Cotton linter is also available in large amounts because it is a by-product of the textile industry. Upscaling of linter for commercial production of cellulosic nanowhiskers requires a supply with little variation in the cellulose content and low impurities content such as seed coat, soil, plant residues, and other contaminants.

3.2. Electronic microscopy

A curled and soft-flat shape was observed in the SEM pictures of the linter (Fig. 1a). The surface was rough with some pits. The average width was 23.04 μm, with a confidence interval of 1.01 μm (Fig. 1b), which is in accordance with reports in the literature (Sczostak, 2009). This curled shape increases the surface area and makes the fiber more reactive than typical cotton fibers. The flat shape of this fiber increases its specific area and favors chemical reactions such as acidic hydrolysis.

The nanocellulose suspension had a white gel appearance (Fig. 2a). Bundles of crystals are depicted in the TEM pictures (Fig. 2b). On average, the whiskers are 177 nm long (ranging from 161 to 193), 12 nm wide (ranging from 10 to 13), and have an aspect ratio (L/D) of 19 (ranging from 20 to 24). The TEM pictures (Fig. 2b) also depict agglomeration of nanocellulose bundles, points with dispersed crystallites, and individual crystals.
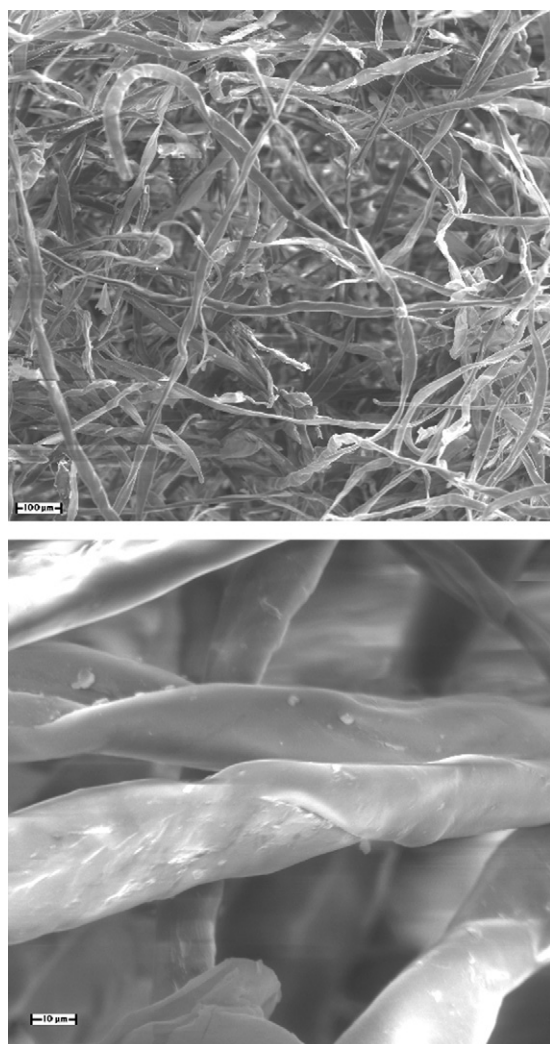

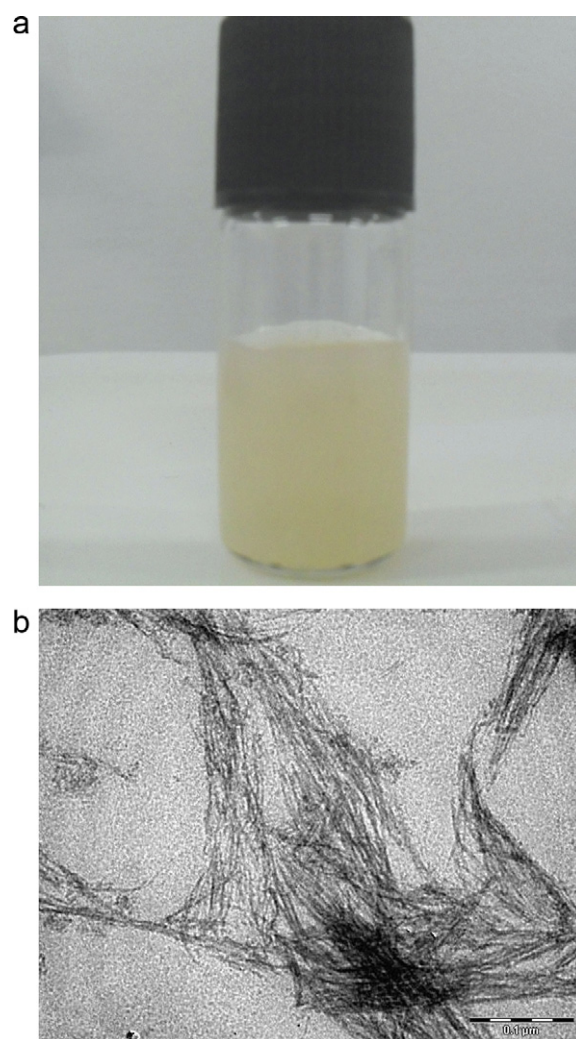**Fig. 1.** SEM pictures of cotton linter cv. Delta Opal.

Fig. 2. Nanocellulose suspension (a) and TEM picture of cotton linter nanowhiskers (b).

a

Onset 46.74 °C
Endset 83.17 °C

Onset 312.92 °C
Endset 360.53 °C

Peak 340.29 °C

dm/dT (1/°C)

b

Onset 50.57 °C
Endset 101.47 °C

Onset 200.95 °C
Endset 235.66 °C

Onset 275.93 °C
Endset 297.66 °C

Onset 383.33 °C
Endset 397.08 °C

dm/dT (1/°C)

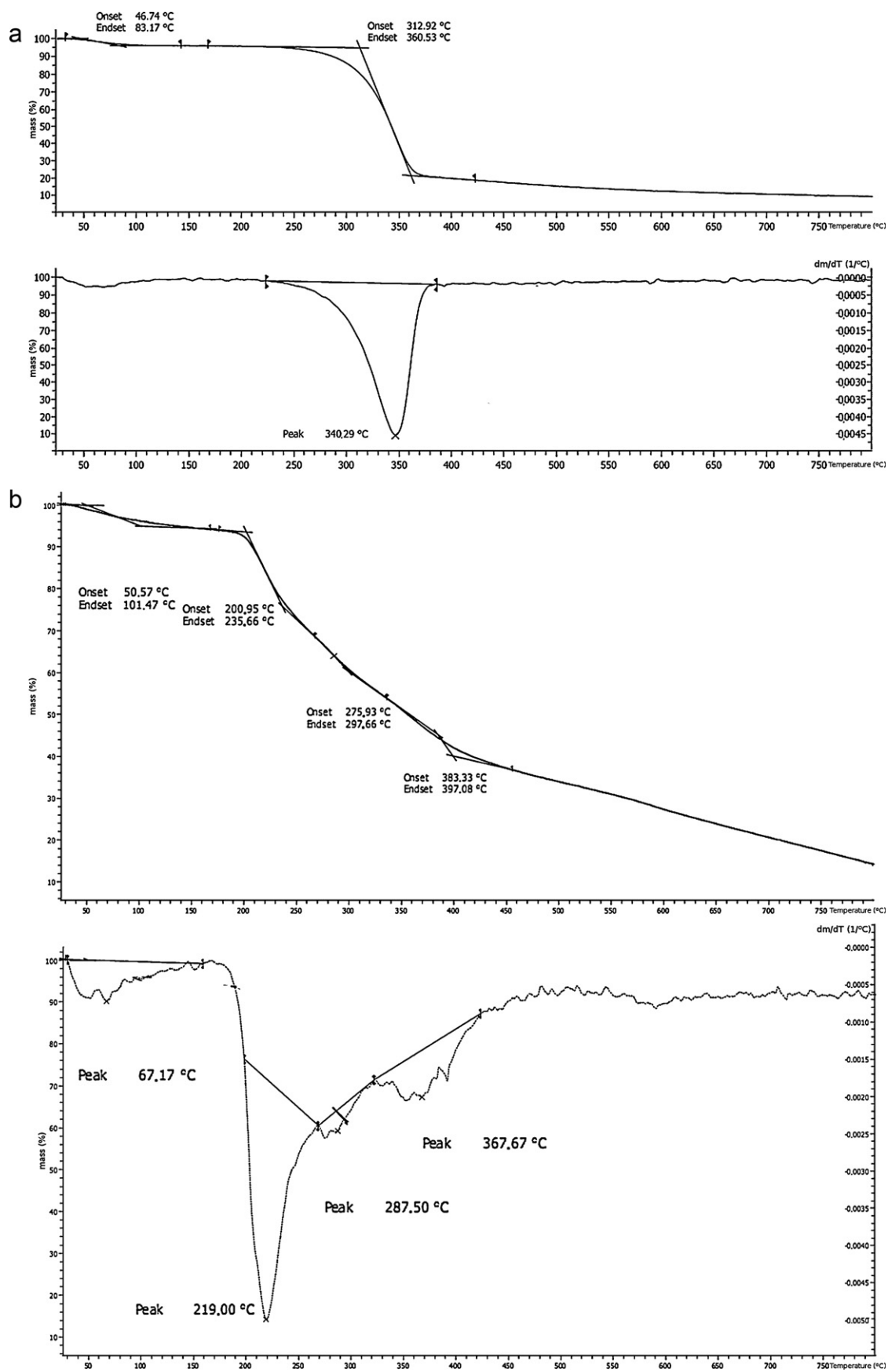Peak 67.17 °C

Peak 367.67 °C

Peak 287.50 °C

Peak 219.00 °C

Fig. 3. Thermal decomposition profile of raw linter (a) and linter nanowhiskers (b), and FTIR spectra (c) of raw linter (bottom) and linter nanowhiskers (top).
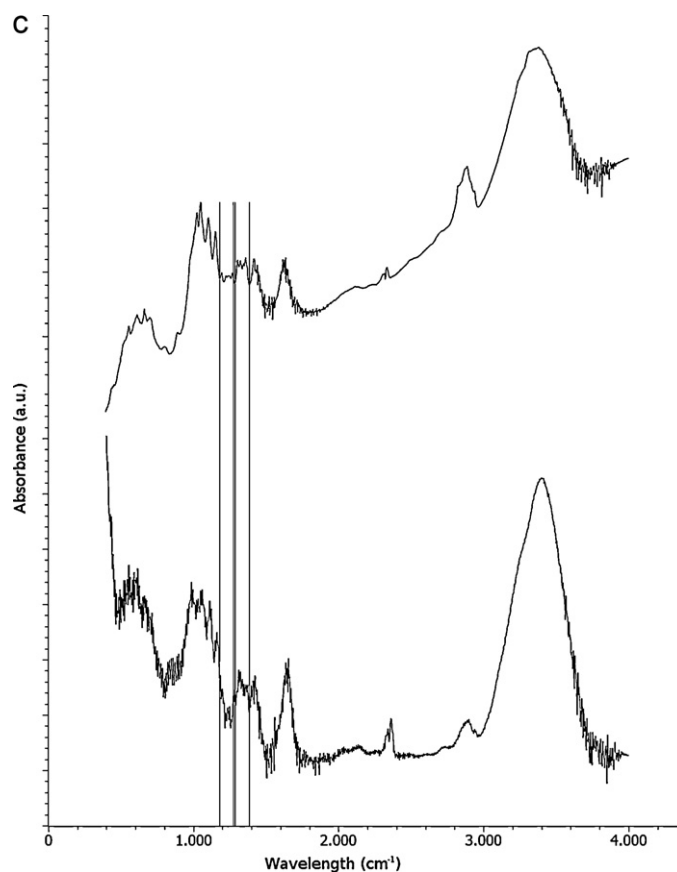
Fig. 3. (*Continued*).

The nanocrystals' dimensions are influenced by the hydrolysis conditions or pretreatments. However, it is widely accepted that the raw material is the most important factor (Beck-Candanedo et al., 2005; Capadona et al., 2009; Eichhorn et al., 2010; Pandey et al., 2010; Silva, Haraguchi, Muniz, & Rubira, 2009). The aspect ratio (L/D) of the crystals extracted from linter is different from those extracted from coconut husks (35–44) (Rosa et al., 2010), sugarcane bagasse (32–64) (Teixeira et al., 2011), sisal (43–60) (Garcia de Rodriguez, Thielemans, & Dufresne, 2006), regular cotton fiber (10–14) (Teixeira et al., 2010), microcrystalline cellulose (11–13) (Capadona et al., 2009; Shanmuganathan, Capadona, Rowan, & Weder, 2010), and flax (*Linum usitatissimum*) (15) (Cao, Dong, & Li, 2007). The aspect ratio of linter nanowhiskers does not overlap with any of those listed, and this raw material is an option if nanocrystals with specific dimensions are required by industry.

3.3. Thermal and FTIR analyses

The decomposition pattern of raw linter is presented in Fig. 3a. There are small weight losses around 45–50 °C related to the moisture. The main T_{onset} of raw linter was at 312.92 °C and the peak was at 340.29 °C. In the nanocellulose (Fig. 3b), the T_{onset} was reduced to 200.95 °C and the main peak was reduced to 219.00 °C. There are also two new weight losses with peaks at 287.50 °C and 367.67 °C, which could be a result of the cellulose sulfonation. This difference may be caused by the removal of the protective waxes and lignin layers from the fiber, as well as the insertion of sulfate groups in the glucose residues (Fig. 3c). There is a reduction of the number of peaks and increasing of the spectrum resolution in the nanocellulose FTIR curve in comparison to the linter FTIR spectrum. There are some peaks between 750 cm^{-1} and 1000 cm^{-1} and other peaks around 1350 cm^{-1} and 1175 cm^{-1}, which indicate the presence of sulfonates in the nanocellulose (Socrates, 2004).

Reduced T_{onset} was also observed in nanocellulose crystals extracted from palm oil (*Elaeis guineensis*) (Fahma, Iwamoto, Hori, Iwata, & Takemura, 2010), coconut husk (Fahma, Iwamoto, Hori, Iwata, & Takemura, 2011), naturally colored cotton fibers (Teixeira et al., 2010), and sugarcane bagasse (Teixeira et al., 2011). In the naturally colored cotton, the reduction from 250–280 °C to 200–205 °C occurred because sulfate groups were inserted and less activation energy was required for the start of the thermal degradation (Teixeira et al., 2010).

3.4. X-ray diffractogram

The diffractograms of linter and nanocellulose had peaks related to the crystallographic plans of cellulose in accordance with the Bragg angles (2θ) with an intensity of 17.422° (plan 1 0 1), 19.169° (plan 1 0 $\bar{1}$), and 26.518° (plan 0 0 2) as indicated by the International Centre for Diffraction Data – ICDD (Fig. 4). The raw linter has a crystallographic pattern very similar to the standard ICDD cellulose, but the pictures are blurring, perhaps due to the presence of non-cellulosic amorphous materials such as fiber extractives (Section 3.1). The nanocellulose diffractogram had a good definition. It had a greater (0 0 2) lattice peak that suggests an increased crystallinity. The higher crystallinity is confirmed by the ICr which was 64.42% for linter and 90.45% for nanocellulose.
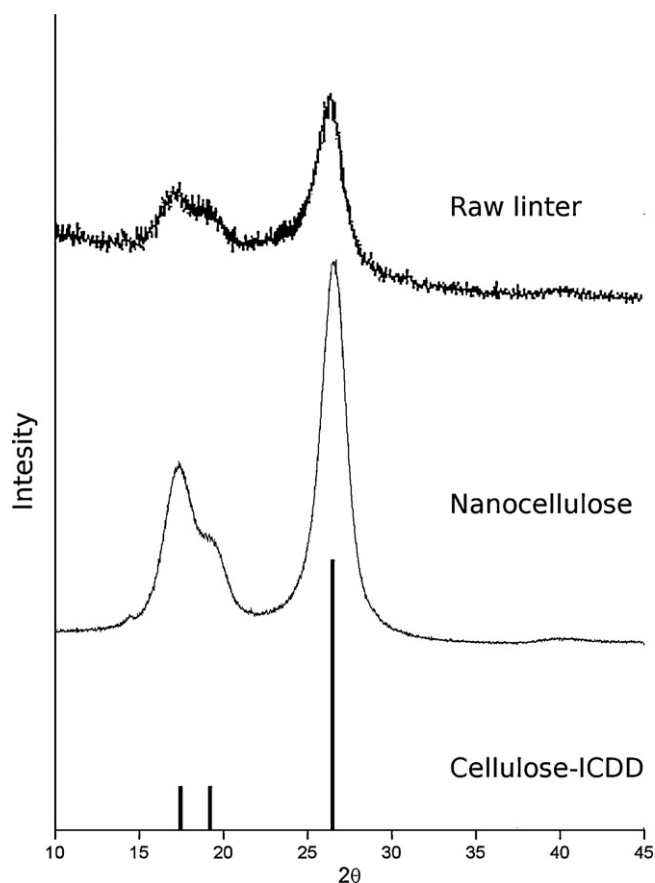
Fig. 4. X-ray diffractogram pattern of untreated linter (top) and cellulose nanowhiskers (middle) in comparison with cellulose X-ray diffraction pattern as ICDD (bottom).

Table 2
Contact angles of raw linter cotton, glass slide and nanocellulose coated glass slide.

Material	Contact angle (mean ± confidence interval)[a]
Raw linter	70.6 ± 3.4°a
Glass	30.6 ± 3.3°b
Nanocellulose coated glass	23.2 ± 4.0°c

[a] Means followed by the same letter do not differ by the Tukeyǐs test at 95% of confidence.
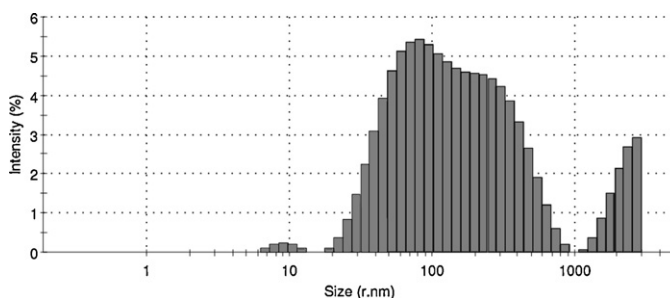

Fig. 6. Particle size distribution of linter nanowhiskers.

The linter crystallinity was increased by 40%, while this increment in other raw materials ranged from 4.6% in medicinal cotton (Teixeira et al., 2010) to 105% in banana fiber (Cherian et al., 2008). After all the different pretreatments for cellulose pulping in these cellulosic sources, the crystallinity may vary from 74% (Cherian et al., 2008) to 91% (Teixeira et al., 2010). Thus, the linter nanocellulose has a high crystallinity, and this property can be important for the composites made of these nanofillers.

3.5. Contact angle

The raw linter has low hydrophilicity (Table 2). This characteristic may be partly explained by the chemical composition of linter (Section 3.1; Sczostak, 2009) and partly by the rough surface (Fig. 1c), which may increase the contact angle due to air bubbles trapped beneath the drop (Spori et al., 2008; Zhang & Kwok, 2003). The thin nanocellulose layer significantly increased the hydrophilicity of the glass surface (Table 2 and Fig. 5). Some reasons for the increased hydrophilicity in the nanocrystals are the exclusion of apolar components, the insertion of polar sulfate groups, and the exposition of OH groups from the cellulose structure.

3.6. Particle size measurement and zeta potential

The zeta potential has a mean value of -45.3 ± 1.4 mV. The suspension of nanocellulose is considered stable because the absolute value is higher than 25 mV (Mirhosseini, Tan, Hamid, & Yusof, 2008). The particle size distribution resulted in three main groups: 0.9% of the particles were around 9.2 nm, 88.6% were around 179.3 nm, and 10.6% were around 2.236 nm (Fig. 6). The particle size measured by light scattering cannot be related precisely to the crystals' diameter and length dimensions of their bundles. However, the first and second groups are similar to the TEM measurements (Section 3.2). If an adequate mathematical treatment is adopted, a light scattering technique can replace TEM for returning a good estimation of nanocrystals' dimensions (Braun, Dorgan, & Chandler, 2008). For linter nanowhiskers, the Smoluchowski algorithm of general purposes was efficient for measuring the linter crystals' dimensions.
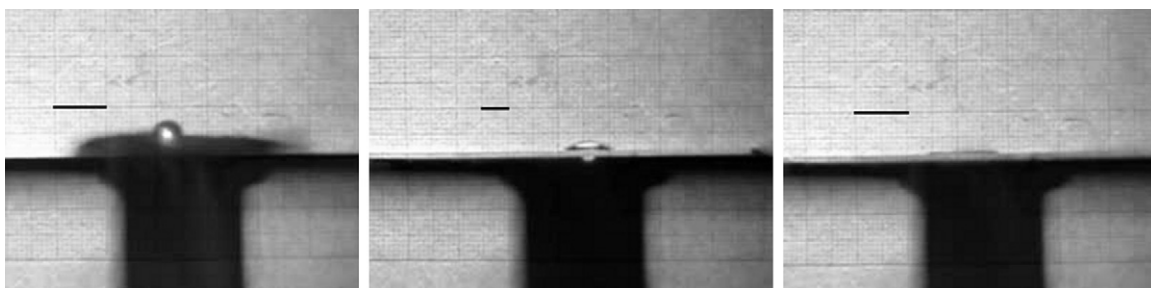

Fig. 5. Contact angle of linter layer (left), glass (center), and nanocellulose coated glass (right) (bar = 1 cm).

4. Conclusions

Cellulose nanocrystals were successfully extracted by hydrolysis from raw cotton linter. The linter nanocrystals have an aspect ratio of 19, crystallinity of 91%, and high hydrophilicity. Their dimensions can be accurately measured by TEM, but light scattering techniques can also be employed for estimating the dimensions. Extraction of nanocellulose from raw cotton linter does not require pulping before the acidic hydrolysis.

Acknowledgments

References

Ardanuy, M., Claramunt, J., García-Hortal, J. A., & Barra, M. (2011). Fiber–matrix interactions in cement mortar composites reinforced with cellulosic fibers. *Cellulose*, 18, 281–289.

Ass, B. A. P., Ciacco, G. T., & Frollini, E. (2006). Cellulose acetates from linters and sisal: Correlation between synthesis conditions in DMAc/LiCl and product properties. *Bioresource Technology*, 97, 1696–1702.

Beck-Candanedo, S., Roman, M., & Gray, D. G. (2005). Effect of reaction conditions on the properties and behavior of wood cellulose nanocrystal suspensions. *Biomacromolecules*, 6, 1048–1054.

Braun, B., Dorgan, J. R., & Chandler, J. P. (2008). Theory and application of light scattering from polydisperse spheroids in the Rayleigh–Gans–Debye regime. *Biomacromolecules*, 9, 1255–1263.

Brígida, A. I. S., Calado, V. M. A., Gonçalves, L. R. B., & Coelho, M. A. Z. (2010). Effect of chemical treatments on properties of green coconut fiber. *Carbohydrate Polymers*, 79, 832–838.

Cao, X., Dong, H., & Li, C. M. (2007). New nanocomposite materials reinforced with flax cellulose nanocrystals in waterborne polyurethane. *Biomacromolecules*, 8, 899–904.

Capadona, J. R., Shanmuganathan, K., Trittschuh, S., Seidel, S., Rowan, S. J., & Weder, C. (2009). Polymer nanocomposites with nanowhiskers isolated from microcrystalline cellulose. *Biomacromolecules*, 10, 712–716.

Castro, K. B., Martins, E. S., Gomes, M. P., Reatto, A., Lopes, C. A., Passo, D. P., et al. (2010). *Caracterização geomorfológica do município de Luís Eduardo Magalhães, Oeste Baiano, Escala 1:100. 000*. Brasília: Embrapa.

Cerqueira, D. A., Rodrigues Filho, G., & Meireles, C. S. (2010). Optimization of sugarcane bagasse cellulose acetylation. *Carbohydrate Polymers*, 69, 579–582.

Chen, W., Yu, H., Liu, Y., Hai, Y., & Zhang, M. (2011). Isolation and characterization of cellulose nanofibers from four plant cellulose fibers using a chemical-ultrasonic process. *Cellulose*, 18, 433–442.

Cherian, B. M., Pothan, L. A., Nguyen-Chung, T., Mennig, G., Kottaisamy, M., & Thomas, S. (2008). A novel method for the synthesis of cellulose nanofibril whiskers from banana fibers and characterization. *Journal of Agricultural and Food Chemistry*, 56, 5617–5627.

Cranston, E. D., & Gray, D. G. (2006). Morphological and optical characterization of polyelectrolyte multilayers incorporating nanocrystalline cellulose. *Biomacromolecules*, 7, 2522–2530.

Eichhorn, S. J., Dufresne, A., Aranguren, M., Marcovich, N. E., Capadona, J. R., Rowan, S. J., et al. (2010). Review: Current international research into cellulose nanofibres and nanocomposites. *Journal of Material Science*, 45, 1–33.

Fahma, F., Iwamoto, S., Hori, N., Iwata, T., & Takemura, A. (2010). Isolation, preparation, and characterization of nanofibers from oil palm empty-fruit-bunch (OPEFB). *Cellulose*, 17, 977–985.

Fahma, F., Iwamoto, S., Hori, N., Iwata, T., & Takemura, A. (2011). Effect of pre-acid-hydrolysis treatment on morphology and properties of cellulose nanowhiskers from coconut husk. *Cellulose*, 18, 443–450.

FAOSTAT Agricultural data. (2012). Production. Crops. Food and Agriculture Organization of the United Nations. http://faostat.fao.org/default.aspx/ Accessed 02.05.12.

Garcia de Rodriguez, N. L., Thielemans, W., & Dufresne, A. (2006). Sisal cellulose whiskers reinforced polyvinyl acetate nanocomposites. *Cellulose*, 13, 261–270.

Ibrahim, M. M., El-Zawawy, W. K., & Nassar, M. A. (2010). Synthesis and characterization of polyvinyl alcohol/nanospherical cellulose particle films. *Carbohydrate Polymers*, 79, 694–699.

Lin, N., Chen, G., Huang, J., Dufresne, A., & Chang, P. R. (2009). Effects of polymer-grafted natural nanocrystals on the structure and mechanical properties of poly(lactic acid): A case of cellulose whisker-graft-polycaprolactone. *Journal of Applied Polymer Science*, 113, 3417–3425.

Medeiros, E. S., Mattoso, L. H. C., Ito, E. N., Gregorski, K. S., Robertson, G. H., Offeman, R. D., et al. (2008). Electrospun nanofibers of poly(vinyl alcohol) reinforced with cellulose nanofibrils. *Journal of Biobased Materials and Bioenergy*, 2, 231–242.

Mirhosseini, H., Tan, C. P., Hamid, N. S. A., & Yusof, S. (2008). Effect of Arabic gum, xanthan gum and orange oil contents on zeta-potential, conductivity, stability, size index and pH of orange beverage emulsion. *Colloids and Surfaces A: Physicochemical and Engineering Aspects*, 315, 47–56.

Oksman, K., Mathew, A. P., Långström, R., Nyström, B., & Joseph, K. (2009). The influence of fibre microstructure on fibre breakage and mechanical properties of natural fibre reinforced polypropylene. *Composites Science and Technology*, 69, 1847–1853.

Orts, W. J., Shey, J., Imam, S. H., Glenn, G. M., Guttman, M. E., & Revol, J. F. (2005). Application of cellulose microfibrils in polymer nanocomposites. *Journal of Polymers and the Environment*, 13, 301–306.

Pääkkö, M., Vapaavuori, J., Silvennoinen, R., Kosonen, H., Ankerfors, M., Lindström, T., et al. (2008). Long and entangled native cellulose I nanofibers allow flexible aerogels and hierarchically porous templates for functionalities. *Soft Matter*, 4, 2492–2499.

Pandey, J. K., Ahn, S. H., Lee, C. S., Mohanty, A. K., & Misra, M. (2010). Recent advances in the application of natural fiber based composites. *Macromolecular Materials and Engineering*, 295, 975–989.

Rånby, B. G. (1949). Aqueous colloidal solutions of cellulose micelles. *Acta Chemica Scandinavica*, 3, 649–650.

Rosa, M. F., Medeiros, E. S., Malmonge, J. A., Gregorski, K. S., Wood, D. F., Mattoso, L. H. C., et al. (2010). Cellulose nanowhiskers from coconut husk fibers: Effect of preparation conditions on their thermal and morphological behavior. *Carbohydrate Polymers*, 81, 83–92.

Sczostak, A. (2009). Cotton linters: An alternative cellulosic raw material. *Macromolecular Symposia*, 280, 45–53.

Segal, L., Creely, J. J., Martin, A. E., Jr., & Conrad, C. M. (1959). An empirical method for estimating the degree of crystallinity of native cellulose using X-ray diffractometer. *Textile Research Journal*, 29, 786–794.

Shanmuganathan, K., Capadona, J. R., Rowan, S. J., & Weder, C. (2010). Bio-inspired mechanically-adaptive nanocomposites derived from cotton cellulose whiskers. *Journal of Materials Chemistry*, 20, 180–186.

Silva, R., Haraguchi, S. K., Muniz, E. C., & Rubira, A. F. (2009). Aplicações de fibras lignocelulósicas na química de polímeros e em compósitos. *Quimica Nova*, 32, 661–671.

Siqueira, G., Bras, J., & Dufresne, A. (2009). Cellulose whiskers versus microfibrils: Influence of the nature of the nanoparticle and its surface functionalization on the thermal and mechanical properties of nanocomposites. *Biomacromolecules*, 10, 425–432.

Socrates, G. (2004). *Infrared and Raman characteristic group frequencies*. New York: John Wiley & Sons., pp. 219–220

Spori, D. M., Drobek, T., Zürcher, S., Ochsner, M., Sprecher, C., Mühlebach, A., et al. (2008). Beyond the lotus effect: Roughness influences on wetting over a wide surface-energy range. *Langmuir*, 24, 5411–5417.

Stelte, W., & Sanadi, A. R. (2009). Preparation and characterization of cellulose nanofibers from two commercial hardwood and softwood pulps. *Industrial & Engineering Chemistry Research*, 48, 11211–11219.

TAPPI. 1993. T 413 om-93. *Ash in wood, pulp, paper and paperboard: Combustion at 900 °C*.

TAPPI. 2000. T 222 om-02. *Acid-insoluble lignin in wood and pulp*.

TAPPI. 2002. T 211 om-02. *Ash in wood, pulp, paper and paperboard: Combustion at 525 °C*.

TAPPI. 2002. T 421 om-02. *Moisture in pulp, paper and paperboard*.

TAPPI. 2009. T 203 cm-99. *Alpha-, beta- and gamma-cellulose in pulp*.

Teixeira, E. M., Bondancia, T. J., Teodoro, K. B. R., Corrêa, A. C., Marconcini, J. M., & Mattoso, L. H. C. (2011). Sugarcane bagasse whiskers: Extraction and characterizations. *Industrial Crops and Products*, 33, 63–66.

Teixeira, E. M., Corrêa, A. C., Manzoli, A., Leite, F. L., Oliveira, C. R., & Mattoso, L. H. C. (2010). Cellulose nanofibers from white and naturally colored cotton fibers. *Cellulose*, 17, 595–606.

Ummartyotin, S., Juntaro, J., Sain, M., & Manuspiya, H. (2012). Development of transparent bacterial cellulose nanocomposite film as substrate for flexible organic light emitting diode (OLED) display. *Industrial Crops and Products*, 35, 92–97.

Vieira, R. M., Beltrão, N. E. M., Lima, R. L. S., & Leão, A. B. (2008). Produção de sementes do algodoeiro. In N. E. M. Beltrão, & D. M. P. Azevedo (Eds.), *O agronegócio do algodão no Brasil* (pp. 509–533). Brasília: Embrapa.

Yang, Q., Fukuzumi, H., Saito, T., Isogai, A., & Zhang, L. (2011). Transparent cellulose films with high gas barrier properties fabricated from aqueous alkali/urea solutions. *Biomacromolecules*, 12, 2766–2771.

Yokoyama, T., Kadla, J. F., & Chang, H.-M. (2002). Microanalytical method for the characterization of fiber components and morphology of woody plants. *Journal of Agricultural and Food Chemistry*, 50, 1040–1044.

Zhang, J., & Kwok, D. Y. (2003). The molecular origin of contact angles in terms of different combining rules for intermolecular potentials. In K. L. Mittal (Ed.), *Contact angle, wettability and adhesion* (pp. 118–159). Utrecht: VSP.

Zhao, X.-B., Wang, L., & Liu, D.-H. (2008). Peracetic acid pretreatment of sugarcane bagasse for enzymatic hydrolysis: A continued work. *Journal of Chemical Technology and Biotechnology*, 83, 950–956.